DRYING TECHNOLOGY, 19(2), 297–312 (2001)

TRANSPORT PROPERTIES OF CELLULAR FOOD MATERIALS UNDERGOING FREEZE-DRYING

Tetsuya Araki,[1] Yasuyuki Sagara,[1] Kamaruddin Abdullah,[2] and Armansyah H. Tambunan[2]

[1]Department of Global Agricultural Sciences,
Graduate School of Agricultural and Life Sciences,
The University of Tokyo, 1-1-1, Yayoi, Bunkyo-ku,
Tokyo, 113-8657, Japan
[2]Agricultural Engineering Sciences, The Graduate School,
IPB, Bogor Agricultural University, P.O. Box 220,
Kampus-IPB, Darmaga, Bogor, 16002, Indonesia

ABSTRACT

The samples of sliced and mashed apples were freeze-dried by controlling their surface temperatures over the usual pressure range of commercial operations. The surface of sliced samples could not be maintained at above 10°C in order to prevent the frozen layer from melting, while that of mashed samples was allowed to heat up to 70°C.

Thermal conductivities and permeabilities were determined by applying the uniformly-retreating-ice front model to the dried layer of the samples undergoing freeze-drying. The values of permeability for the mashed samples were found to depend on the ice-crystallization time during freezing. The results indicated that the drying rate of sliced samples was limited by the transfer rate of water vapor flowing through the dried layer.

A cellular structural model is proposed for predicting the permeability of the dried layer, based on the resistance of the cell membrane to molecular transfer of water vapor.

Key Words: Cellular structural model; Drying characteristics; Mashed apple; Permeability; Sliced apple; Thermal conductivity.

INTRODUCTION

Freeze-drying has had a great impact upon the production of dehydrated foods because of the superior quality of the product obtained, and promises continued expansion of the number of applications. However, the process is only feasible if the cost of production can be lowered by optimum plant operation. Since the rate of freeze-drying is limited by heat and mass transfer rates across a dried material which surrounds the frozen portion of the product, the thermal conductivity and permeability of the dried layer and the effects of processing factors on these transport properties are fundamental information to determine the drying rate.

Various methods, both transient and steady state, have been used to determine the transport properties of freeze-dried food. The transient method was proposed by Lusk et al. (1), Massey and Sunderland (2), Hoge and Pilsworth (3), Stuart and Closset (4), Bralsford (5), Gaffney and Stephenson (6), Sandall et al. (7), and Sagara et al. (8). This method is based on a quasi-steady state analysis of the actual drying data, in which the uniformly-retreating-ice front model was applied to the dried layer of the samples undergoing freeze-drying.

The transport properties of cellular food materials were measured using a steady-state method by Harper and Sahrigi (9) as well as Harper (10). Harper and Sahrigi (9) reported the values of thermal conductivities for freeze-dried apples and pears in the presence of various gases over the pressure range of 1 Pa to atmospheric. Harper (10) presented the effects of gas pressure on permeabilities and thermal conductivities of freeze-dried apples and peaches.

However, available literature on the transient method is limited on the transport properties of cellular food materials such as fresh fruit and vegetables. Particularly, the effects of operating parameters on the drying rate as well as transport properties have not been investigated in depth in connection with the freezing and freeze-drying operations.

The objective of this work are 1) to measure the drying characteristics, thermal conductivity and permeability for sliced and mashed apples, 2) to reveal the influences of freezing rate as well as temperature and pressure

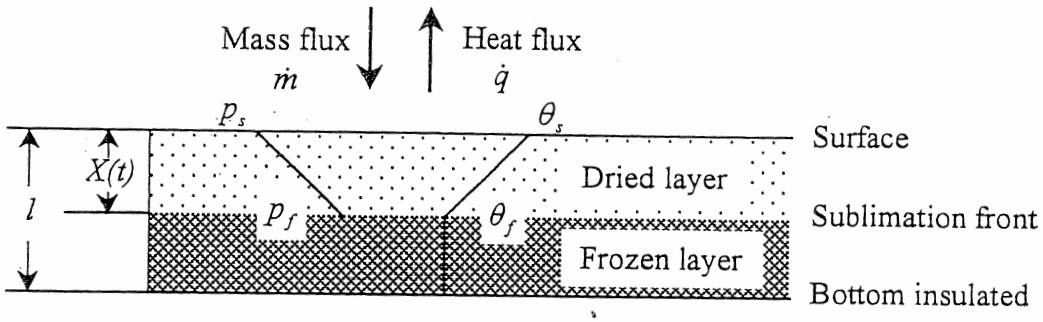

Figure 1. Freeze-drying model for transport properties analysis.

of the dried layer upon these transport properties, and 3) to develop a structural model for predicting the permeability of a cellular food material.

THEORETICAL MODEL

Figure 1 shows a uniformly-retreating-ice front model to determine the transport properties for the dried layer of the material undergoing freeze-drying (Sagara et al.(8)). In the model, the material is assumed to have the geometry of a semi-infinite slab and the dried layer is separated from the frozen layer by the sublimation front. The insulated bottom can be regarded as the center plane of the material heated by radiation from both surfaces of the material. Furthermore, the model has several assumptions; that is, 1) Drying proceeds under a quasi-steady state condition. 2) The change in temperature and pressure in the material, and the movement of the sublimation front are negligible during calculation. 3) The linear distribution in temperature and pressure exists across the drier layer, and the temperature of the frozen layer is uniform and equal to that of the sublimation front. 4) The heat supplied through the dried layer is consumed completely as the latent heat at the sublimation front.

Based on these assumptions, the equations of the heat and mass conservation are introduced, and thus the thermal conductivity and permeability are given as:

$$\lambda = \alpha \rho_w l^2 (\Delta H + \int_{\theta_f}^{\theta_s} C_p d\theta)/N \tag{1}$$

$$K = \beta \rho_w l^2 R T_f / N M_w \tag{2}$$

where,

$$\alpha = (1 - m)/\{(\theta_s - \theta_f)/(-dm/dt)\} \quad (3)$$

$$\beta = (1 - m)/\{(p_f - p_s)/(-dm/dt)\} \quad (4)$$

EXPERIMENTAL

Experimental Freeze-Dryer and Measurement System

Figure 2 illustrates an experimental freeze-dryer and measurement system. The vacuum chamber was a cylindrical enclosure, 492mm in inside diameter by 470mm long, with a Plexiglas door 30mm thick. The transparent door permits visual obervation of the sample during freeze-drying. A rotary vacuum pump was connected through an external condenser and a main valve to the lower part of the vacuum chamber. Both internal and external condensing systems were used to collect and freeze the water-vapor sublimed from the sample and to prevent the moisture from reaching the vacuum pump. A refrigerator for these two condesners is a 1.5kW (R-22 Refrigerant) air-cooled condensing unit with sufficient capacity to reduce the condenser-coil surface temperature to −45 °C. Radiant heat was supplied by an electrically heated plate located above the sample surface. Then the sample surface temperature was controlled with the PID controller by regulating the electrical power to the radiant heater.

The weight loss of the sample was followed by supporting a sample holder on an electronic balance located in the center of the vacuum chamber. This was accomplished by separating a part of load cell from an indicator containing electric circuits. The chamber pressure was measured with both Pirani- and diaphragm type analyzers. All of these data were stored into a personal computer every two minutes.

Sample Holder

Two types of sample holders were prepared for the sliced as well as mashed samples. Figure 3 shows a sample holder used for the sliced samples, equipped with heating plates. The sample was located in the central position of the holder, and its circumference was insulated with fiber-glass. Thus, both sample surfaces were heated by radiant heaters assembled with silicon heaters and copper plates. Temperatures of both surfaces and center of the sample were monitored by using thermocouple probes made of 0.2mm copper-constantan wires.

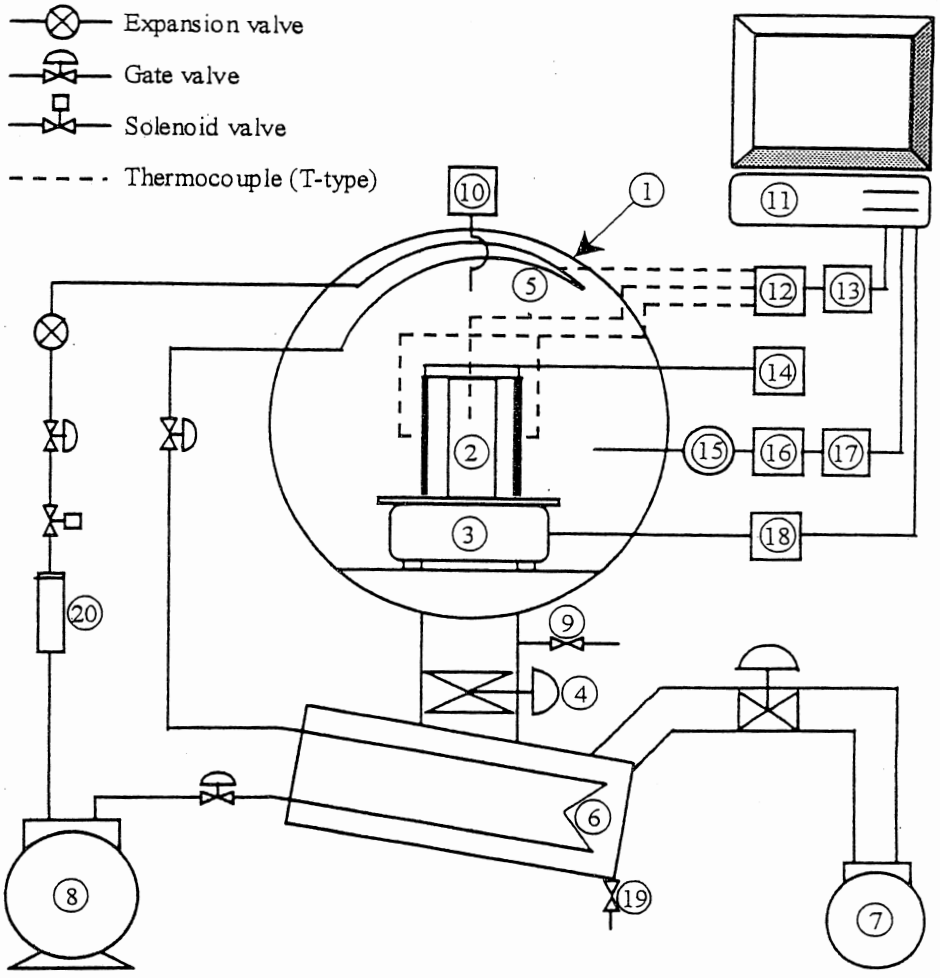

Figure 2. Schematic diagram of the experimental freeze-dryer and measurement system.

Figure 4 shows another type of sample holder prepared for the mashed samples. The sample holder was a Plexiglas dish with 70mm inside diameter and 15mm in height. To promote one-dimensional freezing and freeze-drying, fiber glass insulation was placed around the side of the holder,

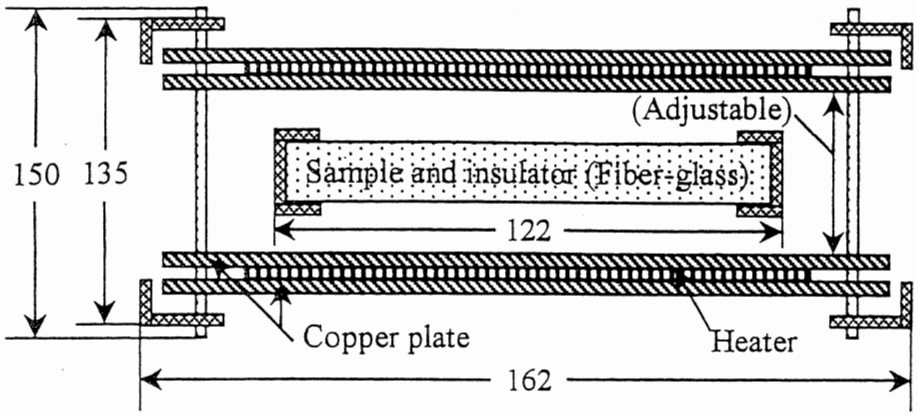

Figure 3. Schematic diagram of the sample holder for the sliced samples.

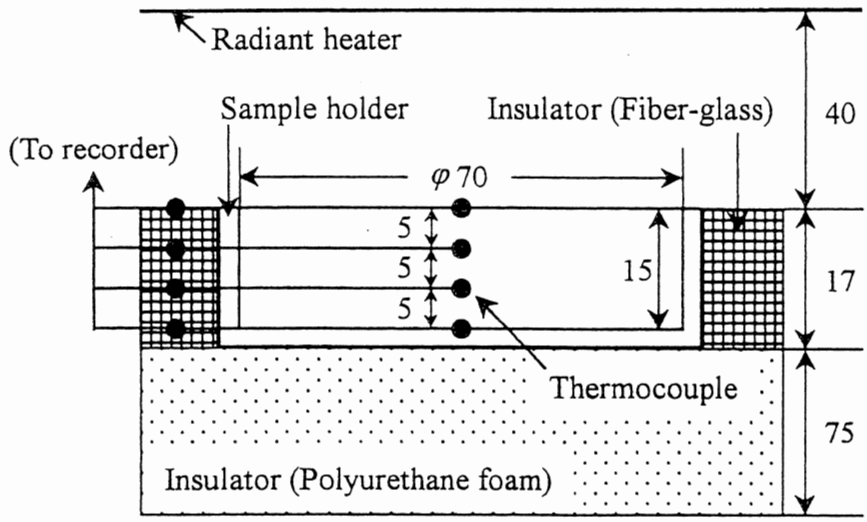

Figure 4. Schematic diagram of the sample holder for the mashed samples.

and its bottom was insulated with a polyurethane foam plate. The change in temperature distribution within the sample was measured with four thermocouple probes. The thermocouple junctions for measuring and controlling the surface temperature were placed just under the exposed surface of the sample.

Materials and Procedure

Both sliced and mashed apples, 15mm thick, were employed as the model material to be dried. Sliced samples were cut out horizontally at the

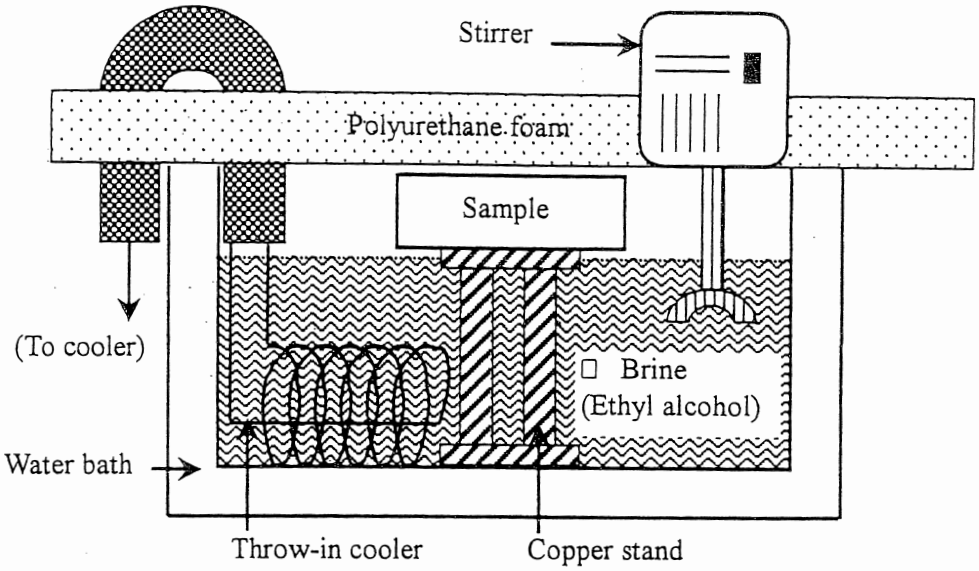

Figure 5. Schematic diagram of freezing apparatus.

equator part, which has the largest diameter in the range from 80 to 90mm. Their cores were removed with a cork borer whose inside diameter was 20mm.

The sample was frozen one-dimensionally by using a cooling copper plate at the surface temperature ranging from −27 to −44°C as shown in Figure 5, and then freeze-dried at a constant surface temperature ranging from −10 to 70°C under the pressure range of 20-30 Pa. The moisture contents of dried samples were determined by Karl Fisher titration method, and the initial moisture contents were calculated based on these data.

RESULTS AND DISCUSSION

Drying Characteristics

Figure 6 shows the drying characteristics obtained for a sliced sample. As shown in the figure, the surface temperature of the sliced sample could not be maintained at a constant temperature of above 10°C in order to prevent the frozen layer from melting. On the other hand, that of the mashed sample was allowed to heat up to 70°C. The results indicated that for the sliced sample the heat supplied across the dried layer was dissipated as not only the latent heat of sublimation, but also sensible heat to raise the temperature of frozen layer.

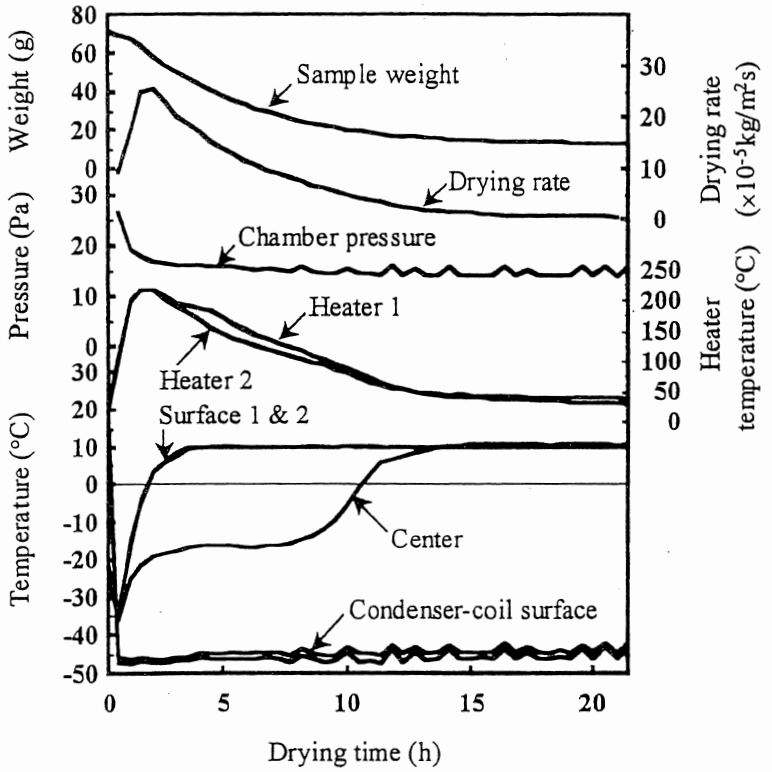

Figure 6. Experimental data obtained during freeze-drying of 15mm thick sliced apple having surface temperature of 10 °C.

Drying rates of these two samples had a tendency to reach the maximum value as the surface temperature reached at a control temperature and after that, to decrease exponentially. However, the maximum drying rate of the mashed sample was about 2.5 times greater than that of the sliced one. This marked difference was interpreted in terms of the larger resistance against the molecular transfer of water vapor by the cellular structure remained in the dried layer of the sliced sample. From these results, the drying rate of the sliced sample was found to be limited by mass transfer rate, while that of mashed by the rate of heat transfer across the dried layer. These facts demonstrated that the value of the permeability should be considered as a critical factor to design the optimum plant operation for cellular food materials.

Transport Properties

Figure 7 and 8 show the plots of the thermal conductivities and permeabilities obtained for sliced samples. As shown in the figure, the

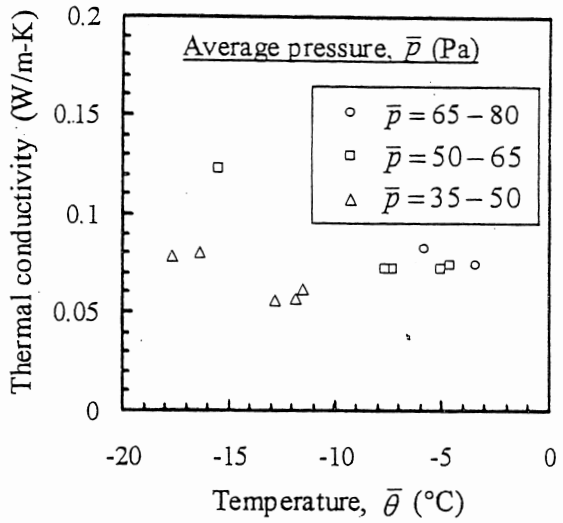

Figure 7. Measured thermal conductivity of sliced samples.

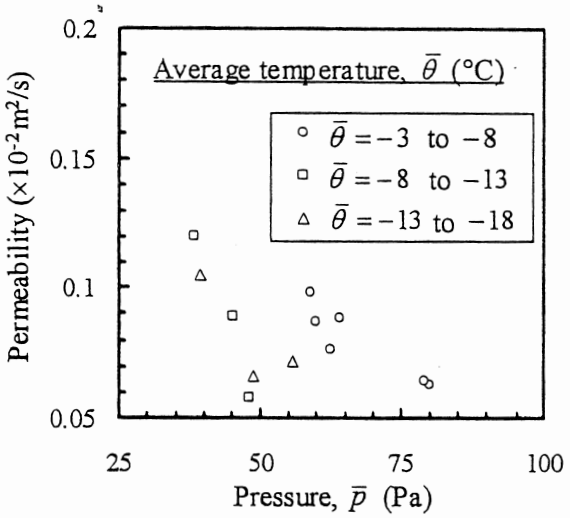

Figure 8. Measured permeabilities of sliced samples.

temperature and pressure dependence of thermal conductivity were not observed apparently, while the permeability showed the tendency to decrease with an increase in the average pressure of the dried layer.

Average values of thermal conductivity were about 2.5 times greater than that of freeze-dried apples presented by Harper (10). His data had been measured against pressure by steady-state method, while in this study the "effective" values of thermal conductivity were measured under the existing conditions of temperature and pressure gradients across the dried layer of the sample undergoing freeze-drying.

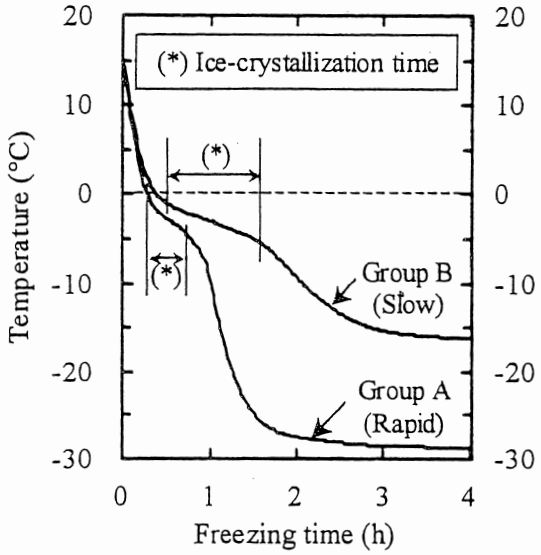

Figure 9. Freezing curves for the mashed samples.

To explain the effect of freezing rate on transport properties, the freezing curves for mashed samples were shown in Figure 9. The changes in temperature at the center during freezing could be regarded as an index of the freezing rate, and based on these indexes the mashed samples were classified into groups A and B. The freezing rate of group A was relatively larger than that of the group B. In order to obtain a quantitative index of the freezing rate, the period between the two inflection points was defined as the ice-crystallization time, based on the primary differential values of these curves.

Figure 10 shows the variation of the permeability against the ice-crystallization time for mashed samples. The linear relationship was found to exist between the permeability and the ice-crystallization time. This tendency was considered to be explained in terms of the larger ice crystals formed in the material as the freezing rate decreased. Hence, the effects of the freezing rate on the transport properties, especially the permeability, were found to be critical for the mashed cellular food materials.

Cellular Structural Model

Sagara (11) developed an approximate method for predicting the structural parameters of the dried layer by considering the dried layer to be a bundle of capillary tubes with the pore space having an equivalent pore

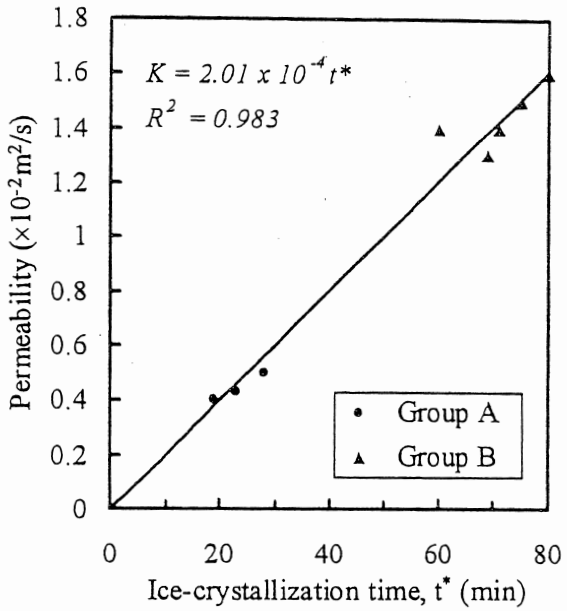

Figure 10. Permeability against the ice-crystallization time for the mashed samples.

radius, porosity and tortuosity factor. The mass flux density of water-vapor flowing through the dried layer may be written

$$\dot{m} = -\frac{KM_w}{RT} grad\ p \tag{5}$$

The expressions for the permeability coefficient of a single capillary tube are taken from Mellor and Lovett (12) as follows:

$$K = \frac{\varepsilon}{\tau} D_k \Omega \tag{6}$$

where,

$$\Omega = \frac{3\pi}{64}\frac{r}{\lambda} + \frac{\pi}{4}\frac{2r/\lambda}{(1+2r/\lambda)} + \frac{1}{1+2r/\lambda} \tag{7}$$

(Poiseulle) (Slip) (Knudsen)

In this equation the value of Ω expresses the total of separate contributions due to Poiseulle's flow, slip flow and Knudsen's flow. The mean free path of a water-vapor molecule λ is given by

$$\lambda = \frac{\kappa T}{\sqrt{2}\pi\sigma_w^2 p} \tag{8}$$

and the Knudsen diffusivity is defined in terms of the pore radius and the average molecular velocity as follows:

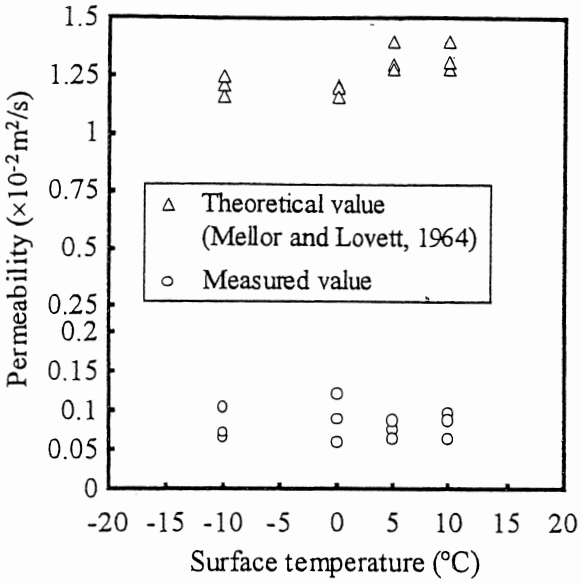

Figure 11. Values of permeability calculated by using equation (6) and measured for sliced samples.

$$D_k = \frac{2}{3}\bar{v}r \tag{9}$$

$$v = \left(\frac{8RT}{\pi M_w}\right)^{1/2} \tag{10}$$

Values of permeability calculated by using the equation (6) were plotted in Figure 11, comparing with those of measured for sliced samples. Under our experimental condition the calculated values were given as a function of average temperature and pressure of the dried layer, and found to be more than 10 times greater than those of measured ones. In order to eliminate this difference, a cellular structural model was proposed as shown in Figure 12.

The model makes several assumptions; 1) All cells are cylinders having the equivalent diameter d_c and length l_c. 2) The n layers of the cell are stacked parallel to the direction of water vapor transfer, within the distance $X(t)$ between the surface and sublimation front of the sample. 3) By using the analogy of electrical circuit, the resistance against the water vapor R_n was determined as the summation of the equivalent resistance R_s of each membrane.

Based on these assumptions, these two structural parameters were introduced to modify the existing theoretical equation (6) for the single capillary tube.

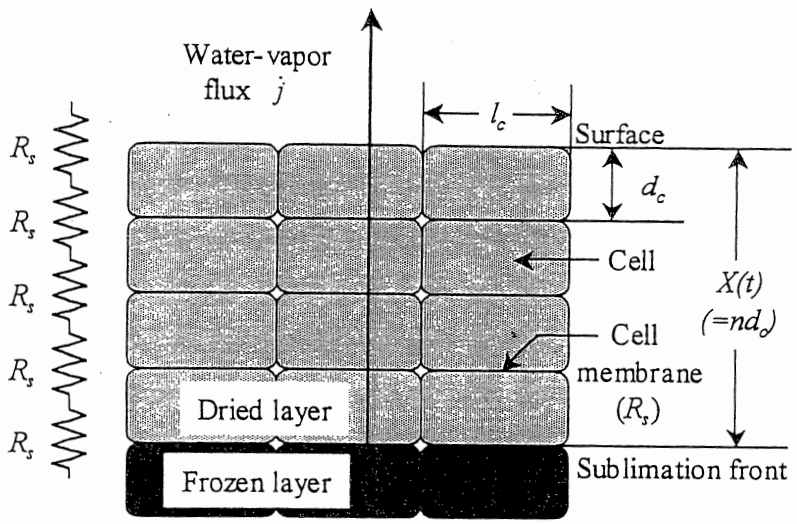

Figure 12. Structural model for cellular food materials.

$$K = \left(\frac{\varepsilon}{\tau} D_k \Omega\right) / R_n \tag{11}$$

$$R_n = (n+1)R_s; \quad R_0 = 1 \tag{12}$$

In the modified model the tortuosity factor τ was assumed to be unity because of the assumption of cells connected in series. According to the equation (7), the value of Ω is considered to be a function of r and T/p since λ is defined in the term of a ratio of absolute temperature to pressure. Therefore, assuming the equivalent pore radius of 150 μm, based on the microscopic observation of the cellular structure in the material, the effects of T/p as well as the terms of each flow on Ω were determined as shown in Figure 13. The value of Ω was found to approach 1 gradually with increasing T/p, indicating the mechanism of Knudsen's flow. Since the values of T/p were in the range of 3.34 to 6.78 under our experimental conditions, the value of Ω can be approximated to be unity, as shown in Figure 13. The values of R_n were in the range of 42.5 to 96.2, and those of R_s were 2.9 to 7.3, and thus the average values were determined to be 71.4 and 4.41, respectively.

As above-mentioned, the parameter R_s can be calculated by carrying out once-time freeze-drying experiment and the microscopic observation of average diameter of all cells, and thus the value of the permeability could be determined for sliced samples. However, the availability of the model depends on some factors such as the average diameter of cells, accuracy of temperature measurement as well as control at the sample surface and the geometrical stability of sublimation front. The sublimation front is

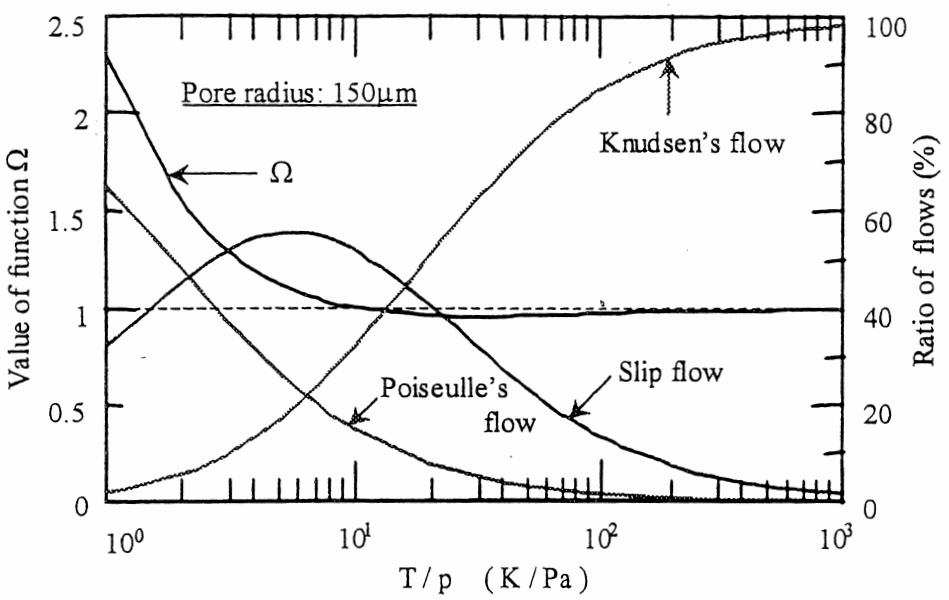

Figure 13. Variation of Ω with T/p and the ratios of flows contribute to Ω.

inclined to lose its stability by thermal edge effect during the later period of sublimation dehydration. To avoid these problems the average diameter of cells should be measured along with the direction of flow for water vapor, and the model is recommended to be applied during the period until the sublimation front reaches about 60% of sample thickness.

The proposed model can be applied to the determination of the permeability for other cellular food materials, and thus its value is useful to calculate the mass transfer rate across the dried layer, and finally, it can be used to design optimum plant operations, or heating program for the surface of cellular food material whose drying rate is limited by mass transfer rate.

NOTATION

c_p = specific heat at constant pressure, J(kg-K)
D_k = Knudsen diffusion coefficient, m^2/s
d = diameter, m
ΔH = latent heat of sublimation of ice, J/kg
j = water-vapor flux, $kg/(m^2\text{-}s)$
K = permeability, m^2/s
l = thickness of slab, m
$\dot{m}$ = mass flux density (mass transfer rate), $kg/(m^2\text{-}s)$

m = the fraction of water remaining, -
M = molecular weight, kg/mol
N = 1 (in radiant heating upon one surface), -
4 (in radiant heatng upon double surface), -
n = number of cells, -
p = pressure, Pa
$\dot{q}$ = heat flux (heat transfer rate), J/(m^2-s)
R = gas constant, (J/mol-K)
R_n = resistance against the water vapor, -
R_s = equivalent resistance of each membrane, -
r = equivalent pore radius, m
T = absolute temperature, K
t = time, s
$\bar{v}$ = average molecular velocity, m/s
$X(t)$ = position of the sublimation front, -

Greek letters

α = constant defined by equation (3), -
β = constant defined by equation (4), -
ε = porosity, -
θ = temperature, °C
κ = Boltzmann constant, J/K
λ = thermal conductivity, W/(m-K) (Equation (1))
= mean free path of the gas molecules, m (Equation (5))
ρ = density, kg/m^3
τ = tortuosity factor, -
Ω = total of separate contributions due to Poiseulle's flow, slip flow and Knudsen's flow. -

Subscripts

c = cell
s = surface
f = sublimation front
w = water vapor

REFERENCES

1. Lusk, G., Karel, M. and Goldblith, S.A., 1964, Thermal Conductivity of Some Freeze-dried Fish, Food Technology, 18(10) pp.1625-1628

2. Massey, W.M. and Sunderland, J.E., 1967, Measurement of Thermal Conductivity during Freeze-drying of Beef, Food Technology, 21(3A) pp.90A-94A
3. Hoge, H.J. and Pilsworth, M.N., 1973, Freeze-drying of Beef, J. of Food Science, 38 pp.841-848
4. Stuart, E.B. and Closset, G., 1971, Pore Size Effect in the Freeze-drying Process, J. of Food Science, 36 pp.388-391
5. Bralsford, R., 1967, Freeze-drying of Beèf, J. of Food Technology, 2 pp,339-363
6. Gaffney, J.J. and Stephenson, K.Q., 1968, Apparent Thermal Conductivity during Freeze-drying of a Food Model, Trans. of ASAE, 11(6) pp.874-880
7. Sandall, O.C., King, C.J. and Wilke, C.R., 1967, The Relationship between Transport Properties and Rates of Freeze-drying of Poultry Meat, AIChE J. 13(3) pp.428-438
8. Sagara, Y. and Hosokawa, A., 1982, Dry Layer Transport Properties and Freeze-drying Characteristics of Coffee Solutions, Proc. Third Int. Drying Symposium (IDS'82), Birmingham, pp.487-496
9. Harper, J.C. and El Sahrigi, A.F., 1964, Thermal Conductivities of Gas-filled Porous Solids, I&EC Fundamentals, 3 pp.318-324
10. Harper, J.C., 1962, Transport Properties of Gases in Porous Media at Reduced Pressures with Reference to Freeze-drying, AIChE J., 8(3) pp.298-302
11. Sagara, Y., 1986, Transport Properties Measurement of Food Sample Undergoing Sublimation Dehydration, Proc. Fifth Int. Drying Symposium (IDS '86), MIT, Cambridge, Vol.1, pp.413-421
12. Mellor, J.D. and Lovett, D.A., Vacuum, Vol. 18, p.625
13. Mellor, J.D., 1978, Fundamentals of Freeze-drying, Academic Press, London, pp.94-128
14. Sagara, Y. and Ichiba, J., 1994, Measurement of Transport Properties for the Dried Layer of Coffee Solution Undergoing Freeze Drying, Drying Technology, 12(5), pp.1081-1103
15. Araki, T., Sagara, Y., Kamaruddin, A. and Tambunan, A.H., 1998, Measurement of Drying Characteristics and Transport Properties for the Dried Layer of Cellular Food Materials Undergoing Freeze Drying, Proc. Eleventh Int. Drying Symposium (IDS '98), Halkidiki, Greece, Vol. B. pp.980-987